UNIVERSITY
OF HARTFORD
ACOUSTICS

A Division of
The Engineering Applications Center
College of Engineering, Technology, & Architecture

Behind the Lip Plane Acoustic Radiation Study of Human Subjects and Head and Torso Simulators

By

Chris Beers
Erik Klein

with
Robert D. Celmer, Ph.D.
Director, Acoustics Laboratory

Report # EAC-2006-15 May 22, 2006

Abstract

Decades of telecommunications technology featured a microphone directly in front of the talker's mouth. However, recent years have seen the development of mobile technologies (such as cellular phones and hands-free devices) that have introduced a microphone located increasingly further from the front of the mouth and closer to the ear. As such, these new devices intrinsically exhibited different behavior than the classic handset. Due to the rapid growth of the mobile device market, new telecommunications transmission standards have yet to be developed for this class of devices. Furthermore, it was unknown how well various head and torso simulators (HATS), which are commonly used in the product development phase of such devices, replicated the actual sound from human speech radiated in this region near the face. To initiate progress on both of these fronts, a study was undertaken to characterize speech sound radiation along the side of the face.

An array of small microphones was used to map the sound radiation pattern simultaneously along the side of the face. These measurements were referenced to a microphone directly in front of the talker's mouth. Measurements were conducted on thirty human subjects and on HATS from three different manufacturers. The overall sound pressure level along the side of the face relative to the front of the mouth was observed. Also, the spectral differences between measurement points along the face relative to the front of the mouth were observed. For both of these measures, the characteristics were observed on humans and compared among humans and HATS models.

Table of Contents

List of Figures and Tables

Purpose

The purpose of the lip plane spectral face mapping was to initiate the process to re-evaluate the current standards for transmission performance for hands-free and behind the lip plane microphone locations for mobile phones.

Background

The current standards for testing the transmission performance for telephones utilize experimental setups that place the microphone directly in front of the mouth. This microphone location is applicable for phones with a larger receiver for which the microphone is directly in front of the user's mouth, as is the case for most land-line telephones. However, this microphone location does not fully replicate the behavior for small cellular phones and hands-free headsets. Many modern cellular phones and hands-free headsets incorporate microphones that are located near the side of the face instead of directly in front of the mouth.

The location of the microphones can be referenced to what is known as the lip plane. The lip plane is defined as the vertical plane through the front of the lips, as shown in Figure 1. The microphone in older telephones is located in front of the lip plane, whereas the microphone in modern cellular phones and hands-free headsets is often behind the lip plane (the region indicated by red arrows in Figure 1.)

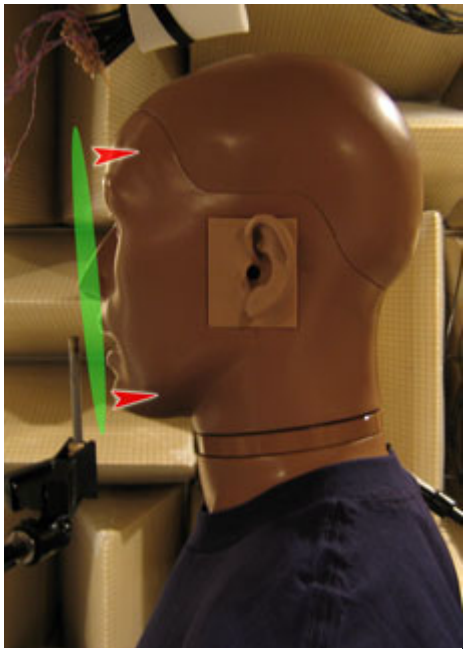

Figure 1. The lip plane is the vertical plane through the lips, as shown in green**.** The red arrows indicate the region behind the lip plane.

The current tests also utilize Head and Torso Simulators (HATS), which model basic human vocal and

auditory systems. HATS are upper body mannequins with built-in ear (transducer microphones) and mouth simulators (output transducer) that are designed to emulate the acoustic speech properties of the average human adult.

In 1991, a study was conducted that attempted to summarize the *Characterization of the acoustic radiation of the human mouth* (R. Ceruti, Special Rapporteur of Q.12/III). This intended to create a CCITT recommendation on Head and Torso Simulators for sound radiation from the human mouth in the far field behind the lip plane region. Five free-field positions were situated 50 cm from the center of the lips in a hemispherical orientation behind the lip plane, as shown in Figure 2. Another microphone was located at the Mouth Reference Position (MRP). The MRP was situated 25 mm in front of the mouth, as seen in Figure 1.

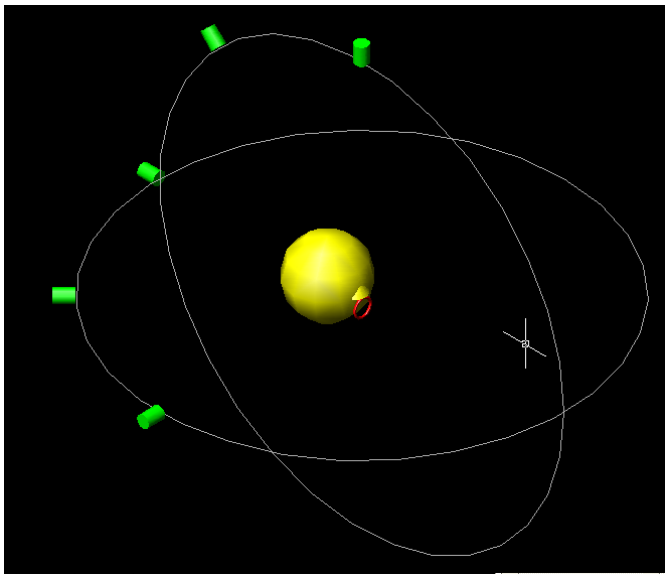

Figure 2. The five free-field microphone locations used in the 1991 CCITT study. All microphones were located 50 cm from the center of the lips.

This study did testing on twelve human subjects and the Brüel & Kjær Type 4227 Artificial Mouth at four separate laboratories. The sound pressure level data at the five free-field positions and at the MRP was analyzed in 1/3 octave bands.

This study provided HATS performance guidelines for all HATS manufacturers. During the time of this study, the cellular phone was not a common electronic device, and the use of hands-free headsets was primarily focused in telemarketing and high-use phone applications.

Within the last 15 years the telecommunications industry has experienced a paradigm shift, which has changed the way we communicate via cellular phones and hands-free headsets.

To test the sound radiation within the relocated microphone region, a near-the-face acoustic map of human speech study was proposed by Dan Foley and Dr. Robert Celmer. This study needed to incorporate human testing, HATS testing, and near-face acoustic field measurements to emulate the location of common cellular phones and hands-free headsets and replication of the free field acoustic field measurements from the 1991 study.

Procedure

Microphone Array Design

An array of small microphones was designed to measure this near-face, behind-the-lip-plane acoustic radiation from speech. A fixed microphone array enabled the simultaneous collection of data at each measurement location and the consistency of inter-microphone spacing among test runs.

MicroElectrical Mechanical Systems (MEMS) microphones were supplied for use in this testing by Akustica, Inc. (Pittsburgh, PA). In general, MEMS devices combine mechanical and electrical components on a single chip, resulting in very small devices. These microphones had a very low profile (4 mm by 4 mm by 1 mm), making them ideal candidates for this measurement. The microphones were omni-directional and had sufficient frequency response and noise floor.

Three major considerations guided the design of the array. First, the array was to span the side of a human face. Horizontally, the microphones extended from the corner of the lips to that portion of the outer ear called the tragus. Vertically, the microphones extended from the cheek bond to the jaw bone. Note that this range covered the area in which microphones are located in most mobile phones and hand-free devices.

Secondly, the integrity of the measurement was a critical array design factor. To that end, the array was designed to be acoustically transparent so the signals would not be significantly affected by the array itself. The small MEMS microphones were attached to a frame of spring steel with a 2-mm diameter and were wired with 32-gage wire, both of which contributed to the acoustical transparency of the apparatus. Also, the array and its hanging mechanism were isolated from any structural vibration paths through the head or cheek. The stability of the array was another important consideration, since a stable measurement device ensured consistency of measurement location.

Finally, it was imperative that human subjects would felt comfortable throughout the test. A comfortable test subject, it was reasoned, resulted in an accurate portrayal of the actual speech patterns of people in non-laboratory settings. The array was thus designed to be comfortable and unobtrusive during testing.

The final design consisted of twelve microphones arranged in a grid as shown in Figure 3. The microphones were arranged in three horizontal rows (top, center, and bottom) of four microphones each. The center row coincided with the line from the corner of the lips to the tragus. Power, signal, and ground leads were soldered to each microphone, and each lead was about 35 cm long. The three leads of each microphone were braided to minimize electromagnetic interference. The signal and ground leads were connected to BNC cables for transmission to the analyzer.

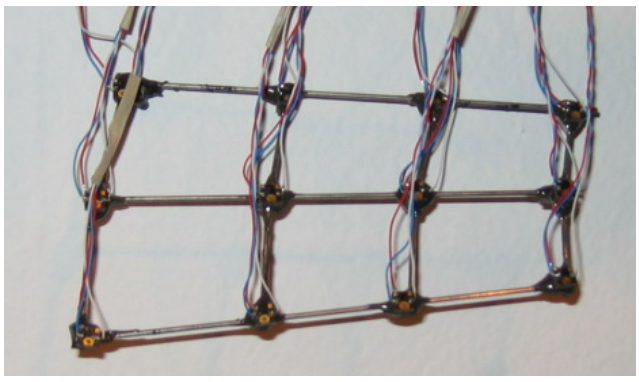

Figure 3. Final construction of microphone array.

Test Setup

Two behind-the-lip-plane regions were characterized in this study: the free-field region 50 cm from the mouth opening to replicate the 1991 Ceruti data, and the near-field region along the side of the talker's face.

In both regions the measurements were analyzed relative to the measurement immediately in front of the talker's mouth, located at the Mouth Reference Position (MRP). The MRP was 25 mm in front of the lip plane, centered vertically and horizontally with respect to the mouth opening, corresponding to the MRP location in the 1991 study. A Brüel & Kjær Type 4136 ¼"-diameter pressure microphone was used to measure the sound pressure level at this location. The pressure microphone was oriented vertically such that its diaphragm was parallel to the propagation direction of the sound. Considering the proximity to the lips, a windscreen was placed over the microphone to reduce "popping" noises that might occur from puffs of air generated by plosive consonants such as "p"s and "b"s.

Due to a limited number of input channels, only four of the five microphone positions from the 1991 study were replicated. Microphone positions A, B, C, and E were chosen for use in this testing. These were positioned 50 cm from the mouth opening above and behind the head as indicated in Table 1 and Figure 4. All microphones were pointed toward the opening of the lips such that their diaphragms were perpendicular to the propagation direction of the sound. A Brüel & Kjær Type 4190 ½"-diameter free-field microphone was used at each position.

Measurement Point	Azimuth Angle from front (in horizontal plane through lips)	Elevation Angle (measured up from horizontal plane)
A	90°	0°
B	135°	0°
C	180°	0°

E	180°	90°

Table 1. Measurement locations for free-field microphones.

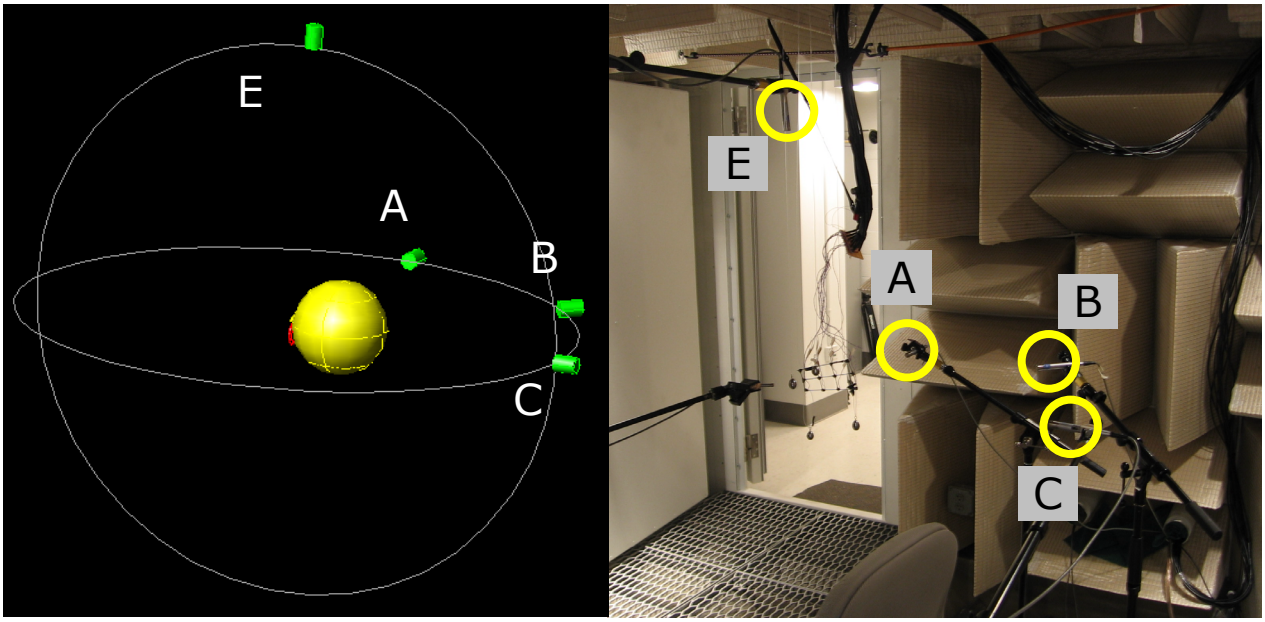

Figure 4. Actual test setup of free-field microphones.

The microphone array was suspended by fishing line from the ceiling, hanging next to the right side of the talker's face. Weights were hung below the array to stabilize the array. The microphone ports faced away from the subject's face. The cables for the microphones were pulled back out of the way, and absorptive material was placed around these cables to minimize any possible acoustic reflections from the cables.

The MRP and free-field microphones were connected via limo cables to the 5/1-channel Input/Output Controller Module Type 7537 of a 17-channel Brüel & Kjær Type Type 3560C PULSE Analyzer. The twelve MEMS microphones on the array were connected via BNC cables to the 12-channel Input Module Type 3038 of the same analyzer. All channels were simultaneously streamed to hard disk at a sampling rate of 22 kHz via the Brüel & Kjær Time Data Recorder.

The test was conducted in the in the Anechoic Chamber of the University of Hartford Acoustics Engineering Laboratory. Prior to the start of testing, the Anechoic Chamber underwent ISO qualification testing for free fields, using the procedures in ISO 3745. The Anechoic Chamber demonstrated qualification for testing in the full frequency range of 1/3-octave bands centered at 100 Hz through 10 kHz.

The room's background sound pressure level was approximately L_P = 17 dBA (re: 20 μPa). A microphone was placed in the chamber and run to an amplifier and speaker outside of the chamber so the test operators could monitor the participants talking. In addition, a walkie-talkie was placed inside the chamber so the operators could communicate with the participants. This two-way communication allowed for efficient operation of the test.

Speech Material

Two main criteria were considered in the selection of speech material for use in the study. First, the material was to contain a wide range of phonemes in the English language. In addition, the material was to replicate easy, natural speech. This criterion again related to the overriding stipulation that the entire test procedure would be a comfortable environment for the test subjects.

Sentences developed for the Hearing In Noise Test, or HINT (Nilsson, Soli, and Sullivan, 1993) met this criteria. HINT was developed to measure sentence speech reception thresholds in quiet and noisy environments. As a part of that test, sets of sentences were developed that replicated the naturalness and phonemic content of human speech. As such, they were ideal for use in the present study. An additional benefit of using these sentences was the availability of a professional audio recording, a feature that was beneficial in the HATS testing. The sentences used in this study were included in Appendix A.

Test Procedure

Approval for the test was secured from the University of Hartford Human Subjects Committee, Dr. Peter Kennedy, Chair. Thirty participants were recruited: fifteen male and fifteen female, with ages ranging from eighteen to twenty-four years. A sample size of thirty was calculated from the desired confidence interval (± 1 dB at 95% confidence) and the expected variance among humans (see Appendix B). The human testing was conducted from 3 April through 5 April 2006.

For each subject, the participant signed an informed consent form and received a nominal monetary compensation. Each person was introduced to the acoustics labs, the anechoic chamber, and the measurement setup. The test procedure was explained in the anechoic chamber to allow for some acclimation of any participant who was not accustomed to the reflection-free environment. Each participant was given the opportunity to ask questions, and the test commenced.

The participant was seated in a comfortable chair, the height of which was adjusted to attain the correct position with regard to the free-field microphone setup. The array was then lowered next to the subject's face. In order to achieve consistent alignment of the array, the participant was asked to move his or her head slightly, and the hanging of the array was adjusted as needed. Adjustment was completed when the array was parallel to the cheek, the array was spaced approximately one centimeter away from the cheek, the front microphone of the center row was at the corner of the lips, and the center row of microphones traced the line from the corner of the lips to the tragus.

Two means were used to ensure that the participant's head did not move. First, a small fishing weight was hung just above the participant's left ear to provide a spatial reference point

for his or her head. Also, the small sheet containing the testing sentences was hung from the ceiling approximately 60 cm in front of the participant, allowing for a visual reference point.

The participant practiced reading the set of sentences several times before recording. This allowed the participant to become familiar with the speech material and speaking in the anechoic chamber. This also provided an opportunity to monitor the loudness of the speech. Although the differences between the microphones and the reference microphone were analyzed, it was nonetheless of interest to achieve approximately the same speech loudness at the MRP for each subject. The goal sound pressure level for this test was L_P = 88 dBA (re: 20 μPa). During this "warm-up" stage, participants were given feedback by the operators regarding their speaking loudness. The participants were asked to adjust their loudness until they spoke at approximately the goal sound pressure level.

At this point, the subjects read through all ten sentences and were recorded. After one recording, an initial analysis was conducted to determine if the speech loudness was close to the goal sound pressure level. After this quick check, the participant was informed whether he or she should talk louder or softer. The subjects then read the sentences again, and another recording was made. After the second recording, the participants were assisted out of the test setup.

HATS from three companies were also tested: Brüel & Kjær Type 4128D, a GRAS KEMAR prototype, and a Head Acoustics HMS II.3. The frequency response of each mouth transducer was determined by exciting the transducer with pink noise and analyzing the output in one-third octave bands. This frequency response data was then used to inverse-weight the professional audio recording of the HINT sentences such that the output of the mouth transducer had equivalent spectral content to the original recording. From this point, the procedure for testing the HATS was analogous to the procedure used in human subject testing, regarding sound

level adjustment and recording the sentences. HATS testing was conducted from 7 April through 11 April 2006.

Analysis

The first stage of analysis consisted of time-averaging the recorded sound files. The files were analyzed in one-twelfth octave bands from 100 Hz to 10 kHz. This analysis was completed in the Brüel & Kjær LabShop software version 10.0, and the data was then exported directly to Microsoft Excel. There were 81 one-twelfth octave bands for each of seventeen microphones for all thirty-three subjects, resulting in over 45,500 data points.

In order to analyze this data efficiently, MATLAB version 7.1 was used. Both the overall sound pressure level (OASPL) and the frequency-dependent sound pressure level (SPL) were of interest. The data from the LabShop software was in pressure-squared, so to calculate the OASPL, the pressure-squared data was summed across all frequencies (for each subject and each microphone) and then converted to decibels. The overall sound pressure level at each array and free-field microphone relative to the MRP microphone was then calculated: $\Delta OASPL = OASPL_{microphone} - OASPL_{MRP}$. The mean and standard deviation of this ΔOASPL was then calculated across all human subjects. Similarly, the pressure-squared data was converted into frequency-dependent SPL, the differences between the microphones and the MRP microphone were calculated at each one-twelfth octave band (ΔSPL), and the mean and standard deviation of the ΔSPL were calculated across all human subjects. For both ΔOASPL and ΔSPL, the 95% confidence limits were calculated from the standard deviation and sample size. The final mean and confidence limits of ΔOASPL was a function of microphone, and the final mean and confidence limits of ΔSPL was a function of microphone and frequency. All spectral results were at least 10 dBA above any noise floor, either ambient or due to signal chain components.

Results

Comparison to Previous Study

The mean ΔSPL spectrum and corresponding confidence limits for this study and the previous study were plotted for each free-field microphone position, as shown in Figure 5.

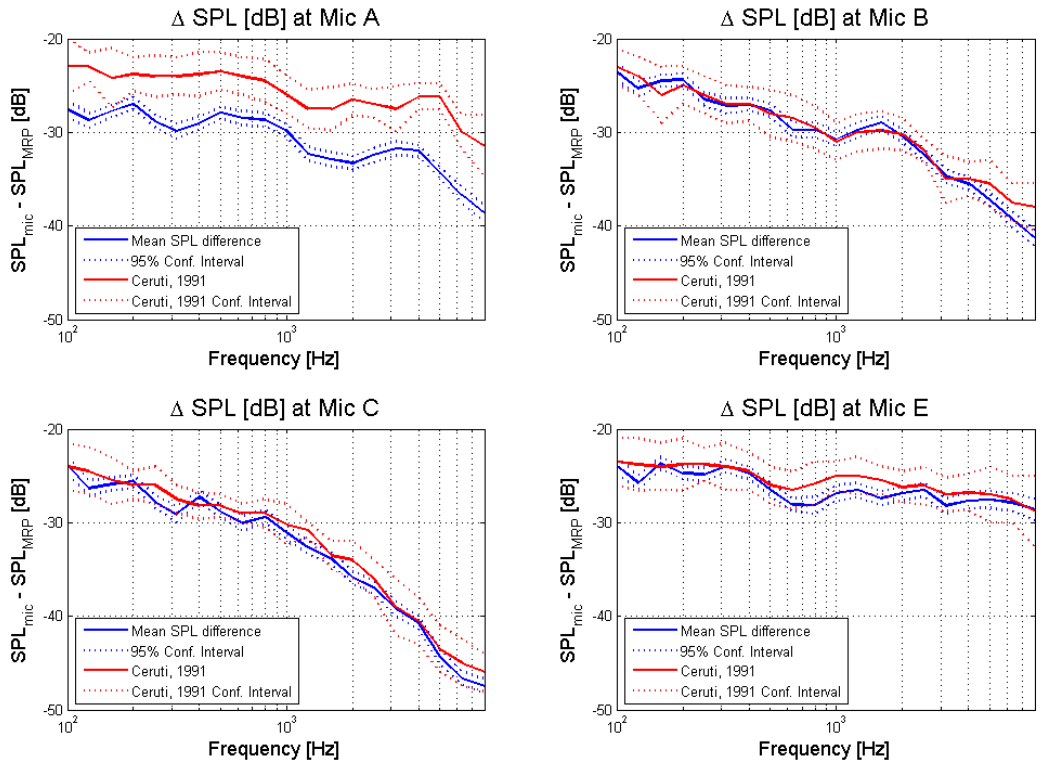

Figure 5. Comparison of measured frequency spectrum (in 1/3-octave bands) between this study (blue lines) and 1991 ITU study (red lines). Mean data shown in a solid line, and 95% upper and lower confidence intervals shown in dotted lines.

Spatial Variation of Overall Sound Pressure Level

The change in ΔOASPL across the span of the array was plotted as shown in Figure 6. This plot represented the data averaged across all human subjects.

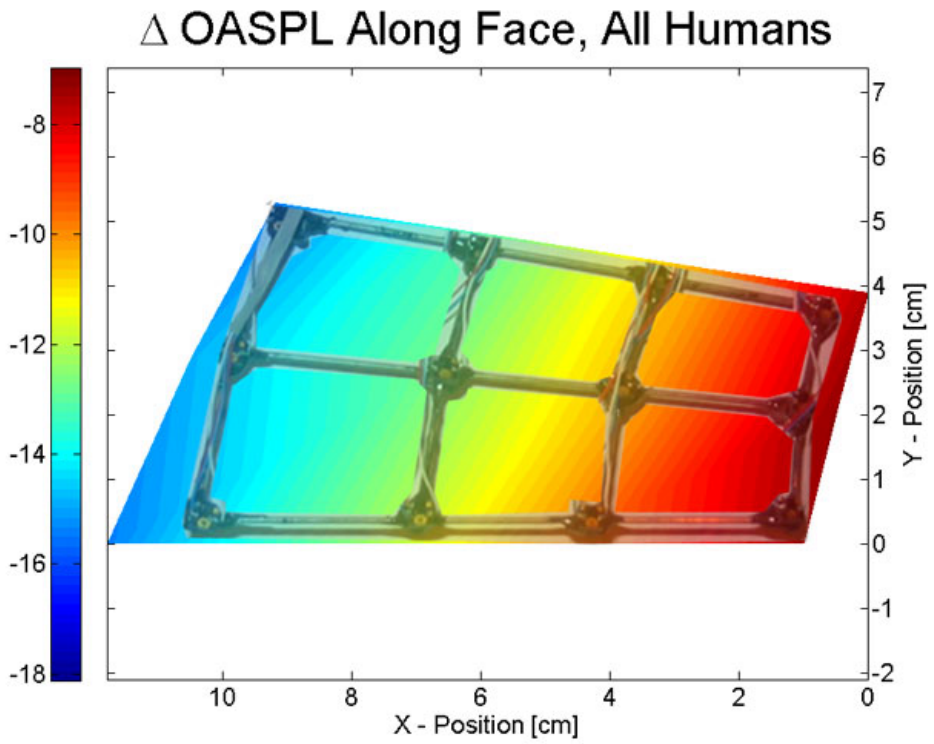

Figure 6. Plot of difference in ΔOASPL as a function of spatial location along the cheek. Colors represented the loudness or softness relative to the MRP microphone. Small differences between the microphone and MRP (i.e., loudest regions) represented by red; large differences between the microphone and MRP (i.e., quietest regions) represented by blue.

This plot was compared with the data measured on the HATS, as shown in Figure 7.

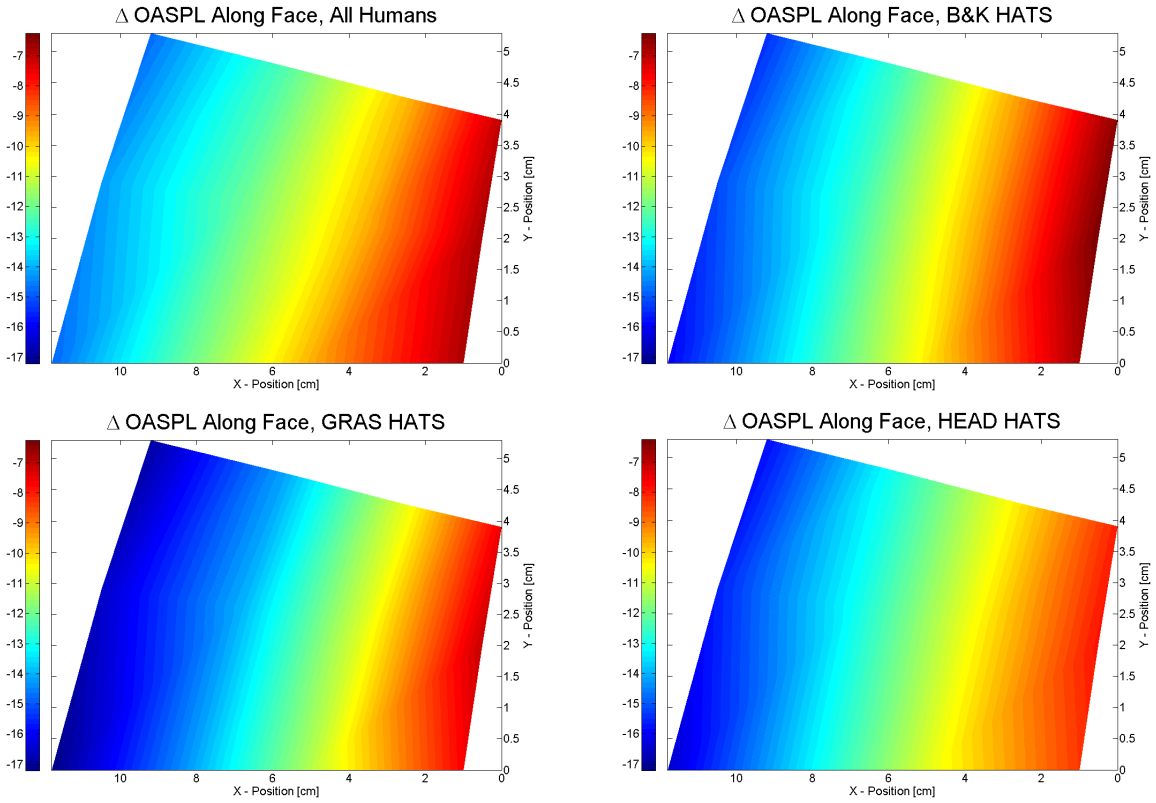

Figure 7. Plot of difference in ΔOASPL as a function of spatial location along the cheek. Colors represented the loudness or softness relative to the MRP microphone. Small differences between the microphone and MRP (i.e., loudest regions) represented by red; large differences between the microphone and MRP (i.e., quietest regions) represented by blue.

Spatial Variance of Spectral Content

The change in the measured spectrum between the microphone on the array and the MRP for microphone positions from the front to the back of the array was plotted as shown in Figure 8. This plot represented the data averaged across all human subjects.

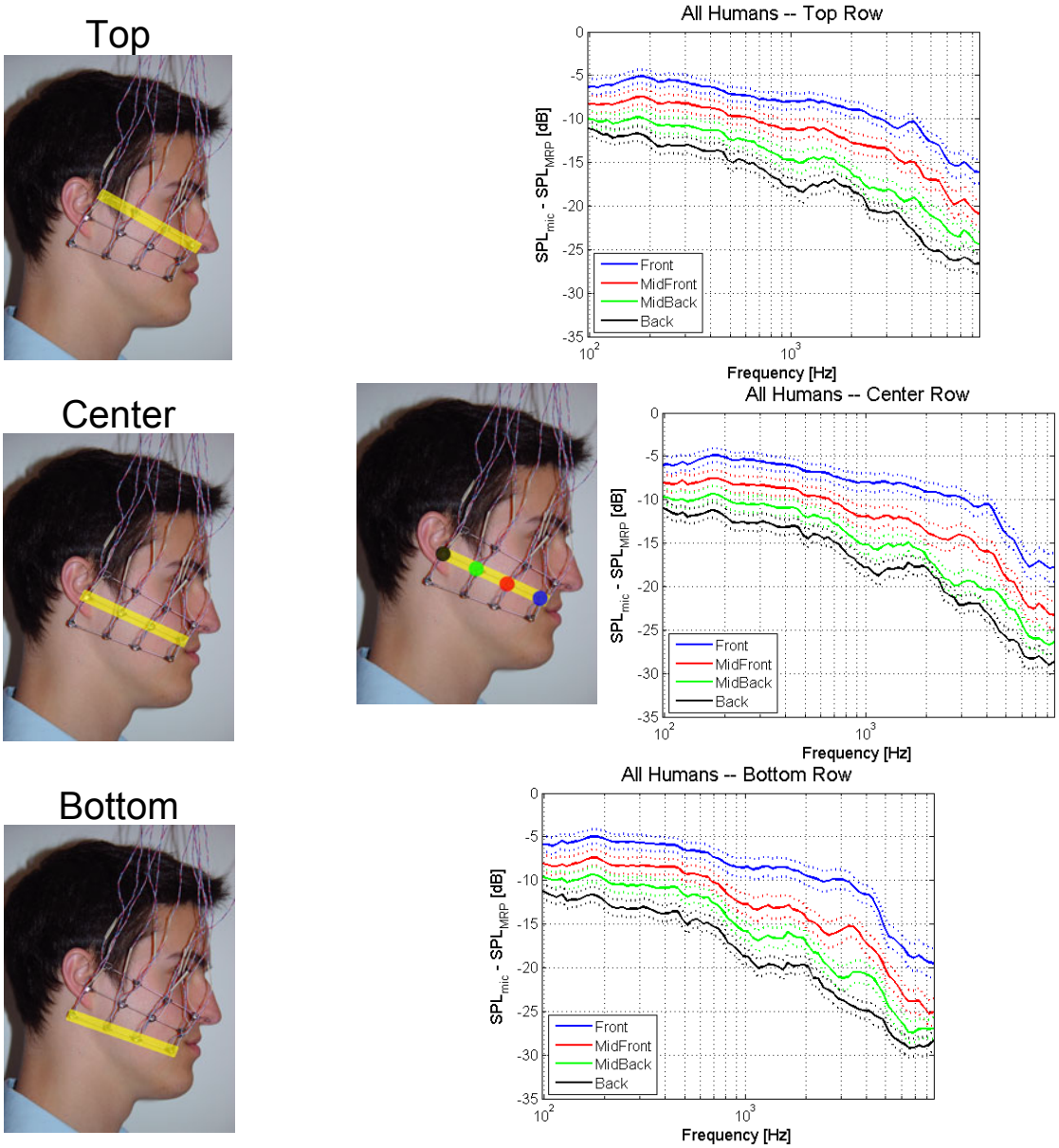

Figure 8. Plot of difference in ΔSPL as a function of spatial location along the top, center, and bottom rows of the microphone array. The colored lines represented the microphone locations along the array from front (corner of lips) to back (tragus), as pictorially indicated adjacent to the center row graph. Mean data was plotted with a solid line, and 95% upper and lower confidence intervals were plotted with dotted lines.

These plots were compared with the data measured on the HATS, as shown in Figures 9 through 11. Confidence limits were not applicable for HATS results because only one HATS was measured for each manufacturer.

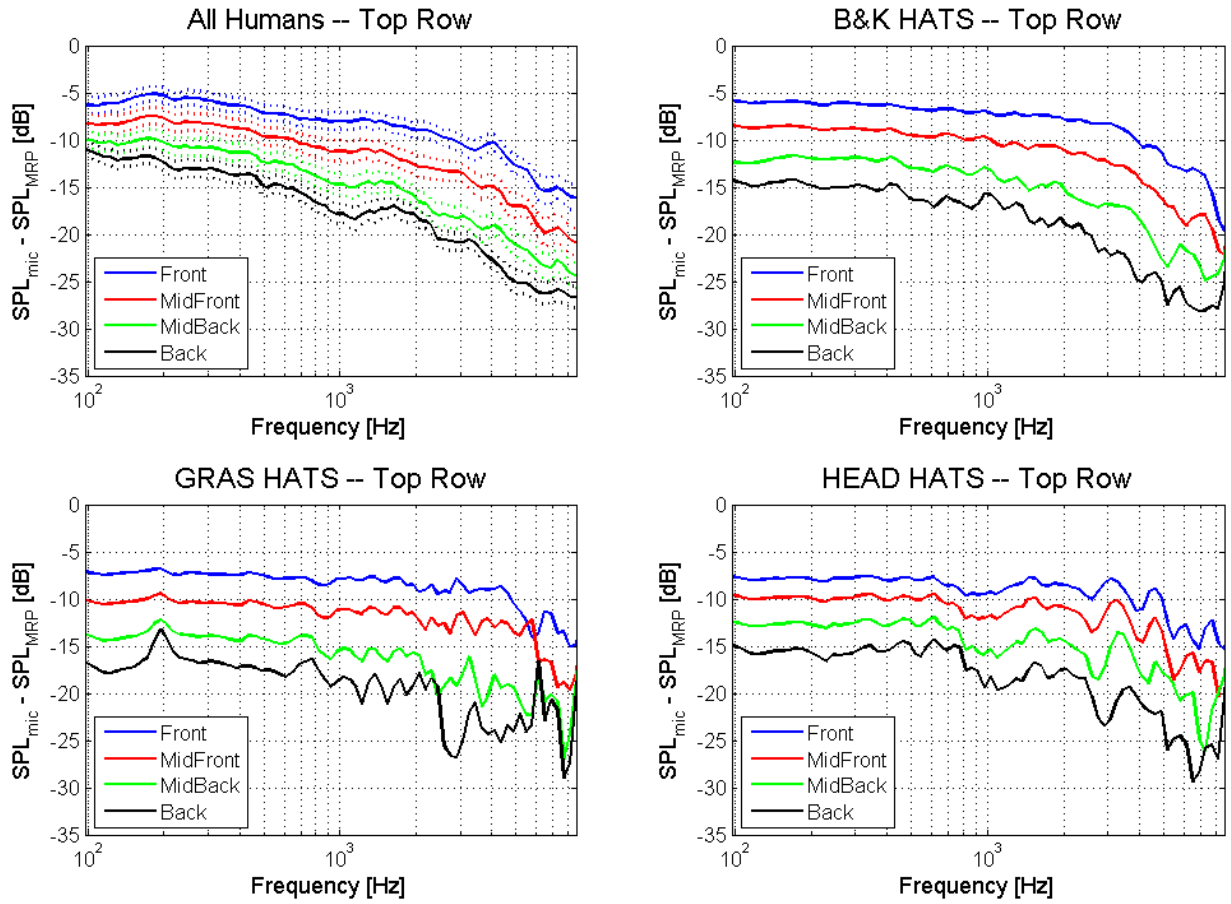

Figure 9. Plot of difference in ΔSPL as a function of spatial location along the top row of the microphone array. The colored lines represented the microphone locations along the array from front (corner of lips) to back (tragus). Mean data was plotted with a solid line, and 95% upper and lower confidence intervals were plotted with dotted lines (confidence intervals applicable only for humans).

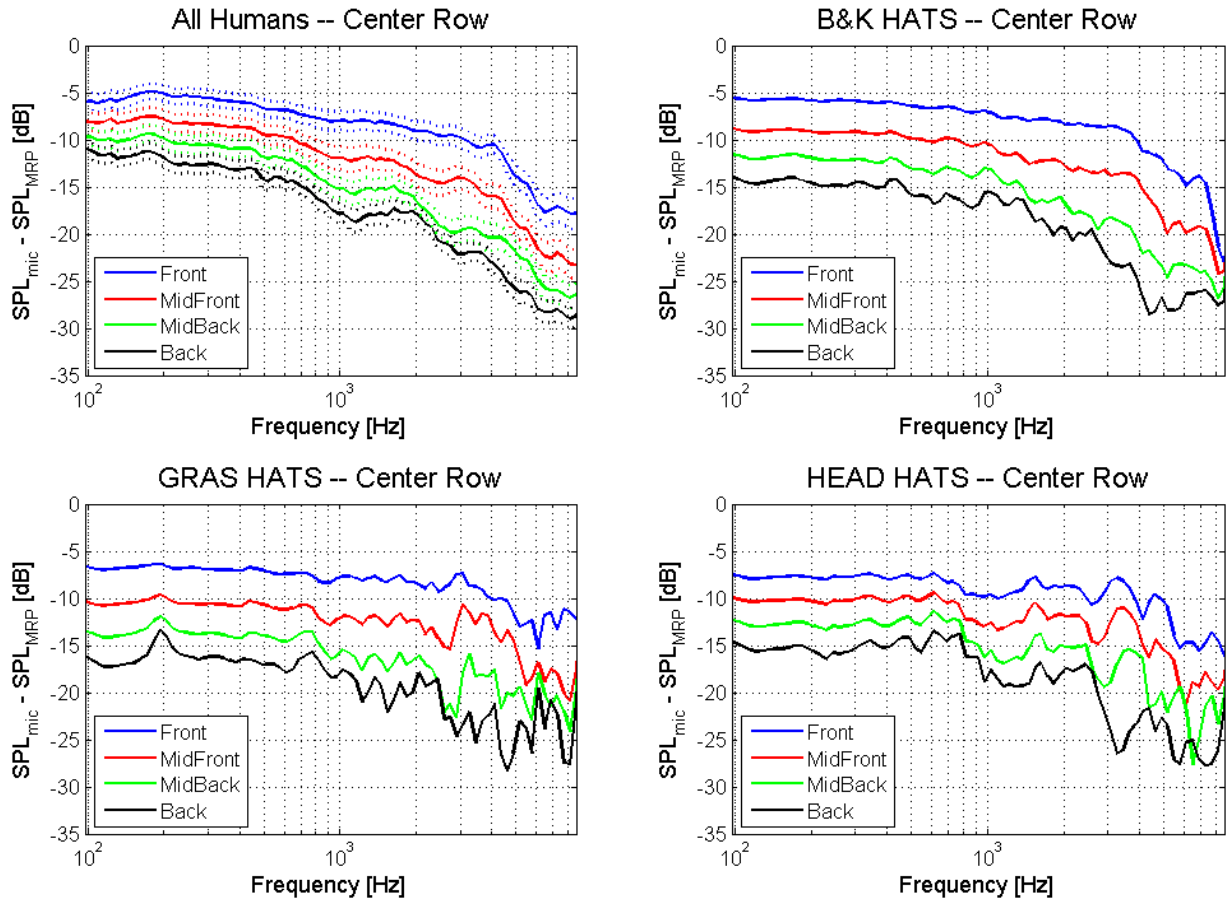

Figure 10. Plot of difference in ΔSPL as a function of spatial location along the center row of the microphone array. The colored lines represented the microphone locations along the array from front (corner of lips) to back (tragus). Mean data was plotted with a solid line, and 95% upper and lower confidence intervals were plotted with dotted lines (confidence intervals applicable only for humans).

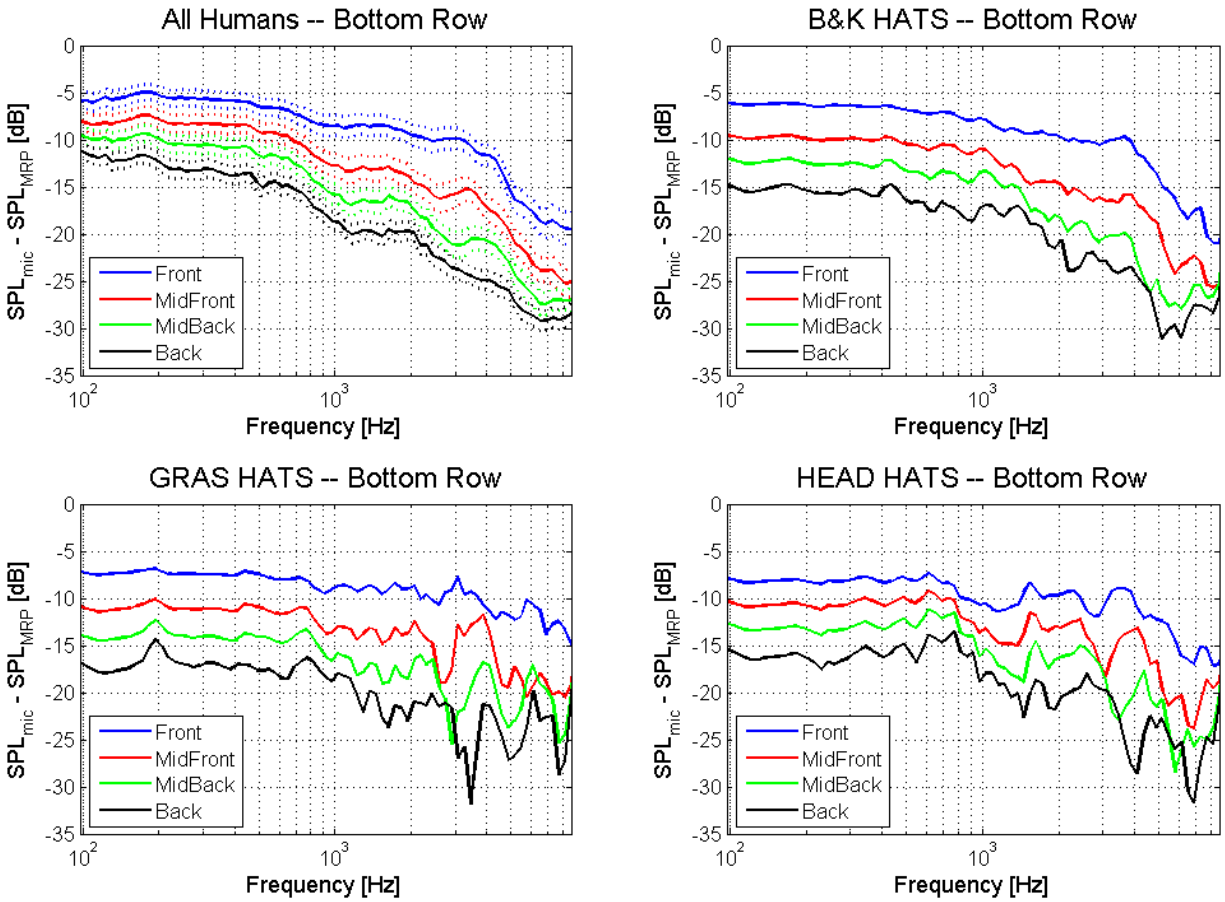

Figure 11. Plot of difference in ΔSPL as a function of spatial location along the bottom row of the microphone array. The colored lines represented the microphone locations along the array from front (corner of lips) to back (tragus). Mean data was plotted with a solid line, and 95% upper and lower confidence intervals were plotted with dotted lines (confidence intervals applicable only for humans).

Discussion

Comparison to Previous Study

The measurements at the 50-cm spherical positions in the free field acoustic speech field closely replicated the 1991 study at the B, C and E positions. The measurements at the A position were lower than the 1991 study, but the cause for this discrepancy has yet to be realized. There was no measurement to replicate the D position from the original study, due to data input limitations. The one-twelfth octave measured data was summed into one-third octave data for a clear comparison. The close correspondence of the data for positions B, C and E confirm the consistency of our experimental setup with the previous voice characterization study in 1991.

Spatial Variation of Overall Sound Pressure Level

The spatial variation plots represented the overall sound pressure level (OASPL) difference with relation to the levels recorded at each location on the microphone matrix face array minus the levels recorded at the mouth reference position (MRP). As shown in Figure 6, the sound pressure level difference is greater the further the microphone location is from the corner of the mouth, which was assumed to be the dominant sound source. Figure 6 shows the overlay of the microphone matrix on the spatial intensity graph for dimensional perspective. This plot clearly shows the relationship between the twelve microphones, three rows of four microphones that comprised the microphone matrix, and the delta sound pressure levels at each position in the near face sound field.

The overall sound pressure level decreased linearly from the corner of the lips to the tragus. This decrease was most significant along this line, whereas minimal variation was observed perpendicular to this lip-tragus axis.

Figure 7 shows the delta OASPL in relation to the positions along the side of the HATS face. For the Brüel & Kjær Type 4128D, this shows a greater delta OASPL at the microphone

positions closest to the ear, compared to the average human speech delta OASPL. The Brüel & Kjær HATS closely approximates the delta OASPL levels recorded as compared to the human testing, especially at the locations near the lip plane. It should be noted that the human difference levels are smallest at the point below the corner of the mouth, this is not replicated as closely with the Brüel & Kjær HATS. The GRAS KEMAR prototype HATS showed a significantly larger difference throughout the face array as compared to the average of the human test subjects. The HEAD Acoustics HMS II.3 HATS shows the greatest OASPL difference at lip plane, but has a uniform difference gradient along matrix array. The Brüel & Kjær HATS most closely matches the trends recorded by the average of the thirty human test subjects.

Spatial Variance of Spectral Content

The variation of the relative spectrum (array microphone – MRP) for humans, as plotted in Figure 8, showed several interesting characteristics. More low-frequency sound energy than high-frequency energy (relative to MRP) was observed at each measurement location. If the radiation from the mouth opening is assumed to be the dominant source, this effect would be expected due to the tendency of low frequencies to diffract more than high frequencies.

The difference between consecutive spectra (front-to-back) was approximately equal below approximately 1000 Hz. Above 1000 Hz, though, the spectra were not spaced equally. For example, at 2000 Hz there was a much smaller difference between the back two microphones than there was between the front two microphones. Around 3000 Hz the difference between consecutive microphones was different for each pair (front to mid-front, mid-front to mid-back, and mid-back to back.) While the exact cause of these unequal spacings above 1000 Hz was not determined, they may have been due to physical features. For example, the wavelength at 2000 Hz is close to 17 cm, which is close to the distance between the tragus and the shoulders.

These characteristics observed in the human data were used to evaluate the accuracy of the HATS responses. As seen in Figures 9 through 11, more low-frequency energy than high-frequency energy was generally noticed for each HATS. Also, inequality in spacing among the various curves was noticed for each HATS. For both of these characteristics, the HATS exhibited similarity to the human characteristic to varying degrees of accuracy.

Also, the rate at which the ΔSPL changed from 100 Hz to 1000 Hz was observed. The human data exhibited a fairly steady decrease. The Brüel & Kjær HATS also demonstrated a steady decrease, but to a lesser extent. The GRAS HATS showed little decrease in this region, and the HEAD HATS displayed a moderate decrease that did not start until around 600 Hz.

In addition, the relative smoothness of the spectra served as an additional indicator of HATS accuracy. The human spectra were generally quite smooth, a feature most accurately replicated by the Brüel & Kjær HATS. The HEAD and GRAS HATS exhibit fairly smooth, flat spectra below 1000 Hz, but the spectra above 1000 Hz were noticeably less smooth than the human data.

In general, the HATS displayed some similarities to human characteristics. While the characteristics were typically in the ballpark of the human data, accuracy can be improved in multiple aspects.

Acknowledgements

The authors extend many thanks to the following people and organizations for their generous support and guidance throughout the course of the study:

Dan Foley, Independent Consultant, Marlborough, MA
Dr. Mike Daley, Akustica, Inc.
Ken Gabriel, Akustica, Inc.
Marty Alexander, Brüel & Kjær Instruments
Greg Bracci, Brüel & Kjær Instruments
Jason Kunio, Brüel & Kjær Instruments
Flemming Vestergaard, Brüel & Kjær Instruments
Gunnar Rasmussen, G.R.A.S. Sound & Vibration
Edward Terrell, G.R.A.S. Sound & Vibration
Dr. Hans Gierlich, HEAD Acoustics
Roger Gutzwiller, HEAD Acoustics
John Bareham, MichTel Communications
Denise Monte, American School for the Deaf
Nick Zacharov, Nokia
Markus Vaalgamaa, Nokia
Steve Graham, Plantronics
Jim Bobisuthi, Plantronics
Osman Isvan, Plantronics
Allen Woo, Plantronics
Dr. Tom Burns, Starkey Labs
Jim Breneman, Pratt & Whitney and University of Hartford
Dr. Peter Kennedy, Chair of Human Subjects Committee, University of Hartford
Scott Metcalfe and the Music Production Department, The Hartt School, University of Hartford
John Williams, University of Hartford
The Thirty Participants

Appendix A: HINT Sentences

HINT sentences – List 25

The boy slipped on the stairs.
New neighbors are moving in.
The girl caught a head cold.
His father will come home soon.
The bus stopped suddenly.
He is washing his car.
The cat caught a little mouse.
They broke all the brown eggs.
The candy shop is empty.
The lady went to the store.

Source:

Nilsson, M., Soli, S. D., and Sullivan, J. A. (**1994**). "Development of the Hearing In Noise Test for the measurement of speech reception thresholds in quiet and in noise," J. Acoust. Soc. Am. **95**, 1085-1099.

Appendix B: Sample Size Calculations

Definitions of key parameters:

n..... sample size
CI ..... confidence interval: interval around the mean (mean ± half-interval) in which there is a (1-α) probability that the true mean actually lies
α ..... probability that the confidence interval does not include the mean
σ ..... population standard deviation
σ′ ..... pre-experiment estimate of population standard deviation
γ..... probability that the CI half-length will (after the experiment is run) be greater than the desired CI half-length

Iterative sample size calculation procedure:

The iterative calculation was seeded with the estimated sample size if the population standard deviation were known $\left(n = \left(z_{1-\alpha/2} \frac{\sigma'}{(CI)/2} \right)^2 \right)$. This sample size was n_1, and to calculate the next step (n_2), two parameters were needed: $t_{\text{1-}\alpha/2\ ;\ \text{n1-1}}$ and $\chi^2_{\text{1-}\gamma\ ;\ \text{n1-1}}$. The subsequent iterative sample sizes were then calculated according to $n_{i+1} = \left(t_{1-\alpha/2;n_i-1} \frac{\sigma'}{(CI)/2} \right)^2 \left(\frac{\chi_{1-\gamma;n_i-1}}{n_i - 1} \right)$. This formula was iterated until the sample size converged, which usually occurred within about five steps.

The population standard deviation was expected to be somewhere in the 1.5 dB – 2.5 dB range, and it was desired to report the data to ± 1 dB at α=0.05 (i.e., 95% confidence). A risk of 0.01-0.05 was reasonable to achieve this desired confidence interval half-length. The sample sizes for the corresponding combinations of settings were calculated as shown in Table A1.

α	σ estimate (σ') [dB]	Desired CI Half-Length [dB]	γ	Sample Size
0.05	1.5	1	0.05	17
0.05	2	1	0.05	26
0.05	2.5	1	0.05	37
0.05	1.5	1	0.01	20
0.05	2	1	0.01	29
0.05	2.5	1	0.01	41

Table A1. Calculated sample sizes for various combinations of confidence on mean, estimated population standard deviation, desired confidence interval half-length, and risk of not achieving desired confidence interval half-length.

The estimated sample sizes ranged from 17 to 41, so it was decided to arrange for a sample size between 20 and 30. There were more than 30 volunteers, but only 30 were allowed to participate due to financial constraints. These volunteers were evenly divided between males and females.

Source:

Hahn, Gerald J., and William Q. Meeker. *Statistical Intervals: A Guide for Practitioners*. John Wiley & Sons, Inc., 1991, New York.